Plasmonics
https://doi.org/10.1007/s11468-024-02373-7

RESEARCH

Surface Plasmon Transmission Line Based on Folded Stepped Grooves and Spiral-Shaped Structures

Yu-Xin Cui[1] · Jing-Yi Zhang[1] · Lin Li[1] · Yan-Yan Kong[1] · Guo-Ping Zhang[1]

Received: 11 March 2024 / Accepted: 22 May 2024

Abstract
In this paper, a novel coplanar waveguide (CPW) spoof surface plasmon polariton (SSPP) transmission line (TL) is firstly proposed. The equivalent circuit model is established to analyze the effects of the folded stepped groove and spiral-shaped structure. The investigation based on the equivalent circuit model indicates that the dispersion curves can be easily controlled by changing the inductance brought by the etched grooves and spiral structure. The proposed SSPP has a lower cutoff frequency, stronger field confinement, and smaller system size. The proposed SSPP TL is designed, fabricated, and tested, providing experimental demonstration for the design and analysis. The measured S-parameters and electric field distributions indicate that the designed SSPP structure enhances the electric field confinement ability, while achieving miniaturization of SSPP TL.

Keywords Spoof surface plasmon polariton (SSPP) · Coplanar waveguides (CPW) · Dispersion curve

Introduction

Surface plasmon polaritons (SPPs) are a special type of electromagnetic (EM) wave mode with strong field constraints [1]. According to Maxwell's equations, SPPs are excited at the interface of two media with opposite dielectric constants, which can propagate along the interface but exhibit exponential decay in other directions [2]. SPPs exhibit excellent field confinement properties, and have garnered widespread attention in the fields of nanophotonics and plasmonics over the past few decades. However, in the lower terahertz, millimeter-wave, and microwave bands, the behavior of metals is that of a conductor rather than a plasmonic material, which limits the further development of SPP-based devices [3].

To apply the outstanding physical properties of SPPs into terahertz and microwave engineering, the concept of spoof SPPs (SSPPs) supported by periodic subwavelength structures was developed [4]. In 2004, the first SSPP was realized by a square metal hole array [5]. In SSPP structures, ultra-thin SSPP structures, also known as SSPP waveguides or SSPP transmission lines (TLs) [6, 7], have new advantages over traditional microwave media, such as low crosstalk [8], miniaturized packaging [9], and customizable dispersion [10]. In 2014, an ultrathin metal corrugated SSPP transmission line (TL) was proposed [11].

However, in the microwave and terahertz frequency bands, electromagnetic wave transmission lines are limited by wavelength. Through strong field confinement, the electromagnetic wave field can be localized to the subwavelength scale, achieving precise control over the subwavelength scale. In order to achieve strong field constraints, people have made a lot of efforts. In [12], the field confinement of SSPPs is controlled by proposing a glider-symmetric double-layer (D-L) spoof surface plasmon polariton (SSPP) structure. In [13], a novel planar SSPP waveguide with a fishbone corrugated groove structure is proposed to control the field constraints of SSPPs. Nevertheless, according to the working principle of typical SSPP TLs [14], if stronger field constraints are expected in the millimeter or sub-terahertz band, much larger spaces are required. In [15], although the SSPP TL adopts a miniaturized single-sided structure, to achieve a cutoff frequency below 700 GHz, a width larger than 40 μm is required. In conclusion, there exists a contradiction between achieving strong field confinement and

✉ Lin Li
lilin_door@hotmail.com

1 The Key Laboratory of Intelligent Textile and Flexible Interconnection of Zhejiang Province, School of Information Science and Engineering, Zhejiang Sci-Tech University, Hangzhou 310018, China

Published online: 04 June 2024

miniaturizing the geometric dimensions of spoof SPP TLs, which may be a critical limitation in practical applications.

In [14], the plot of field distribution was observed, and based on the dispersion analysis of spoof SPPs, it was concluded that there is a negative correlation between the field constraint ability and the cutoff frequency. However, to our knowledge, there is currently no direct SSPP equivalent model proposed, which may greatly limit the further application of SSPPs.

In this paper, a novel SSPP TL developed from coplanar waveguide (CPW) is firstly proposed. In comparison to the conventional uniform slotted SSPP TL unit cells, the proposed SSPP TL in the paper adopts a folded stepped slot and a spiral-shaped strip. An equivalent circuit model is established to analyze the effects of the folded stepped slot and spiral-shaped strip. The investigation of the CPW SSPP based on the equivalent circuit model indicates that the dispersion curves can be easily controlled by modifying the inductance brought by the stepped slots and the spiral-shaped strips. This new type of CPW SSPP exhibits lower cutoff frequency, stronger field confinement capability, and smaller SSPP system size. A CPW-based SSPP structure is designed based on the methods derived from the model analysis to simultaneously achieve strong field confinement and miniaturization of the SSPP TL.

Theory and Design Principle

The conventional SSPP unit cell is shown in Fig. 1, where the metal film portion is represented in gray and the dielectric substrate portion is represented in white. The CPW waveguide shown has a line width of w_{ma}, a coupled gap of w_{pa}, and a period of p_a. Each groove structure consists of two strip-shape grooves with the length of l_{sa} and the gap of w_a, etched on both sides of the CPW grounds. The substrate in Fig. 1, and all the following examples in this paper, is FR4, with a thickness of 0.8 mm, a dielectric constant of 4.4, and a loss tangent of 0.02.

For the periodic structures, their electromagnetic characteristics can be described by their unit cells. The dispersion curve can be drawn from the scattering matrix calculated by the circuit model of the cell. In order to gain a deeper understanding of the mechanism of the proposed SSPP unit, we established equivalent circuit models for different unit cells using mixed distribution and lumped circuit components.

The equivalent circuit model of conventional SSPP unit is shown in Fig. 1. The transmission lines with impedance Z_1 and electrical length θ_1 represent the two CPW lines with a width of W_{ma} and a length of $p_a/2$. The two grooves are modeled by the two inductors of L. The two transformers in Fig. 1 describe the electromagnetic coupling between the CPW lines and the etched groove structure. The turn ratios of two transformers can be extracted using the method proposed in [16].

In the equivalent circuit model, the current and voltage are defined as the current flowing through a conductor and the potential difference between the conductor and ground, respectively. For the periodic structures, the relationship between the input (V_n, I_n) and output (V_{n+1}, I_{n+1}) can be calculated, namely the voltage and current of the unit cell. The voltage and current of the unit cell meet the following relationship.

$$V_{n+1} = V_n e^{j\beta p}, I_{n+1} = I_n e^{j\beta p} \tag{1}$$

where β is the propagation constant.

The transfer matrix, also known as the *ABCD* matrix, can be used to describe the input–output relationship between adjacent unit cells in a periodic structure.

$$\begin{pmatrix} V_n \\ I_n \end{pmatrix} = \begin{pmatrix} A & B \\ C & D \end{pmatrix} \begin{pmatrix} V_{n+1} \\ I_{n+1} \end{pmatrix} \tag{2}$$

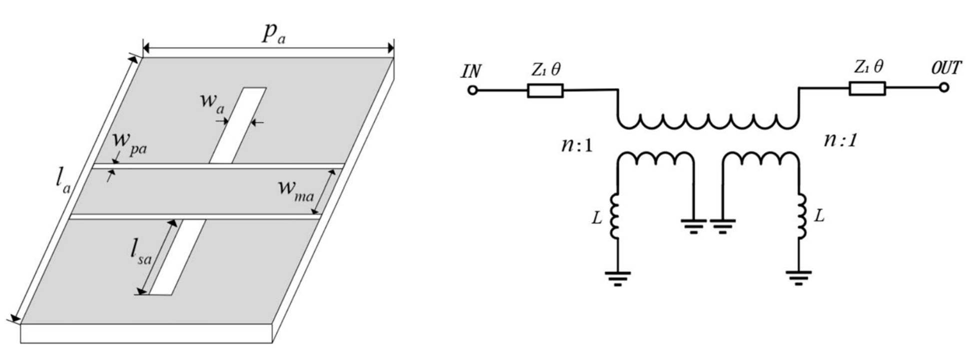

Fig. 1 Conventional SSPP unit cell and its corresponding equivalent circuit

Due to the symmetrical structure proposed in this article, the propagation constant β should satisfy the following relationship:

$$\cos(\beta p) = A \tag{3}$$

By utilizing the circuit parameters of the proposed equivalent circuit model, the *ABCD* matrix can be calculated as follows:

$$\begin{pmatrix} A & B \\ C & D \end{pmatrix} = \begin{pmatrix} \cos^2\theta - \sin^2\theta - \frac{\omega L \sin\theta\cos\theta}{2n^2 Z_1} & 2jZ_1 \sin\theta\cos\theta + \frac{j\omega L\cos^2\theta}{2n^2} \\ \frac{2j\sin\theta\cos\theta}{Z_1} - \frac{j\omega L\sin^2\theta}{2n^2 Z_1^2} & \cos^2\theta - \sin^2\theta - \frac{\omega L\sin\theta\cos\theta}{2n^2 Z_1} \end{pmatrix} \tag{4}$$

By combining Eqs. (1), (2), (3), and (4), the relationship between the inductance L and propagation constant β can be obtained as follows:

$$\beta = \frac{1}{p}\cos^{-1}(A) = \frac{1}{p}\cos^{-1}\left(\cos^2\theta - \sin^2\theta - \frac{\omega L\sin\theta\cos\theta}{2n^2 Z_1}\right) \tag{5}$$

where ω is the angular frequency.

As seen from Eq. (5), the increase of L leads to the decrease of A, resulting in a larger β. In other words, the larger the L, the smaller the cutoff frequency of the dispersion curve, and also the better the field confinement.

To further reduce size occupancy and enhance field confinement capability, one way is to increase L by changing the width of the groove gap. In addition, using a spiral-shaped structure can also increase L. We propose the SSPP unit cell as shown in Fig. 2.

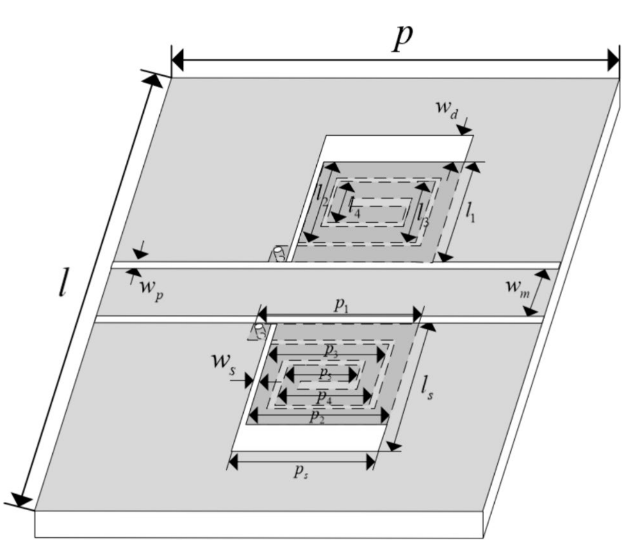

Fig. 2 The proposed SSPP unit cell

Unlike conventional SSPP TLs, the groove structure we proposed consists of a narrow groove and a wider groove, forming a folded stepped groove. The length of the narrow groove is l_s, the gap is w_s, the length of the wide groove is p_s, and the width is w_d. In addition, to further control the dispersion curve, metal through holes and spiral-shaped strip structure is used. The lengths of each part of the spiral-shaped strip from the outside to the inside are l_1, l_2, l_3, and l_4 and the widths are p_1, p_2, p_3, p_4, and p_5, respectively. By utilizing these additional structures to form a CPW structure, better signal transmission and prevention of signal interference can be achieved, thereby improving the overall performance of the system.

Due to the additional inductance caused by changing the slot structure and adding a spiral-shaped strip, we update the equivalent model by adding two additional inductors with the value of ΔL as shown in Fig. 3.

In order to further verify the conclusion of Eq. (5), Fig. 2 preliminarily compares the electromagnetic simulated dispersion curves of SSPP unit cells under different total inductance values L_{total}, and analyzes the simulation results using the SSPP unit intrinsic mode solver in the commercial software CST Microwave Studio. Place the unit in the air box, set the boundary conditions in the x-axis direction as periodic boundaries, and set the y-axis and z-axis directions as ideal PEC boundaries. The dimension parameters in Fig. 2 are set as follows: $l_s = 9$ mm, $w_s = 0.15$ mm, $p_s = 7$ mm, $w_d = 2$ mm, $l_1 = 7$ mm, $l_2 = 5.7$ mm, $l_3 = 4.4$ mm, $l_4 = 3.1$ mm, $p_1 = 8$ mm, $p_2 = 6.7$ mm, $p_3 = 5.4$ mm, $p_4 = 4.1$ mm,

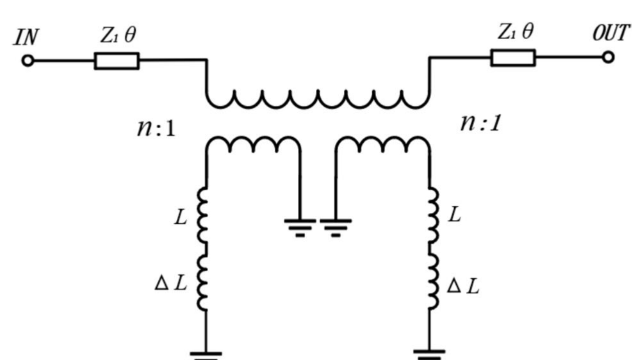

Fig. 3 The equivalent circuit model of proposed SSPP unit cell

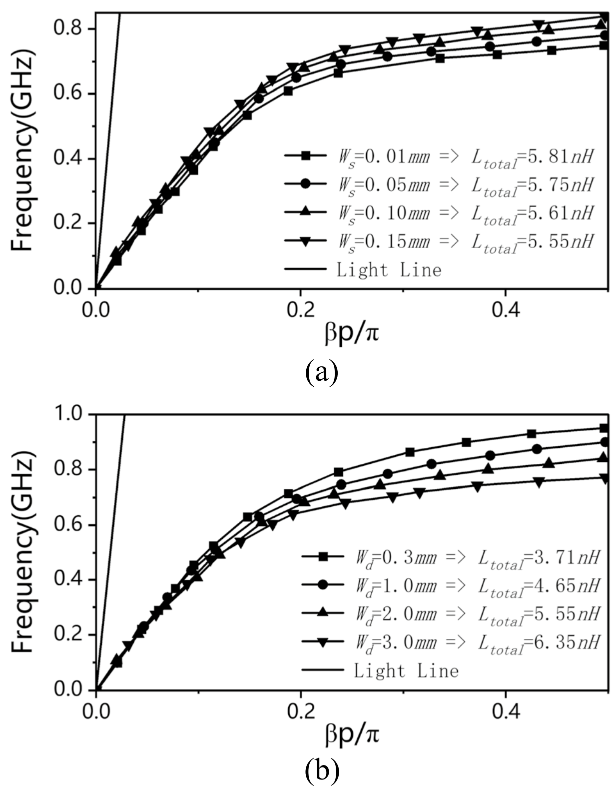

Fig. 4 The dispersion curves with different total inductance L_{total}. **a** Different w_s result in different values L_{total}. **b** Different w_d result in different inductance values L_{total}

$p_5 = 2.8$ mm, $w_p = 0.15$ mm, $w_m = 2.65$ mm, $l = 55$ mm, $p = 25$ mm. In Fig. 4a, w_d is set to be 2 mm and the four values of w_s are 0.01 mm, 0.05 mm, 0.10 mm, and 0.15 mm.

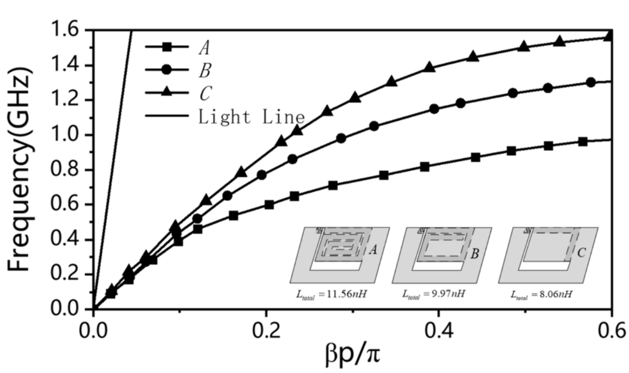

Fig. 5 The dispersion curves with different turns of a spiral-shaped structure

In Fig. 4b, w_s is set to be 0.15 mm and the four values of w_d are 0.3 mm, 1 mm, 2 mm, and 3 mm.

As shown in Fig. 4, the proposed SSPP exhibits a typical SPP response. The dispersion curve approaches the light line at lower frequencies, but gradually moves away at higher frequencies. As mentioned earlier, the larger the L, the lower the cutoff frequency, and the more obvious the SSPP response, resulting in stronger field constraints.

Another way to control the dispersion curve is to add a spiral-shaped strip structure. To investigate the influence of this structure, the EM simulation dispersion curves under different turns of spiral-shaped structure are compared in Fig. 5.

The total inductance values corresponding to the three spiral-shaped strip structures shown in Fig. 5 are 11.56 nH, 9.97 nH, and 8.06 nH, respectively. Obviously, the proposed SSPP corresponds to the structure A shown in Fig. 5. It can be seen from the figure that the larger the number of turns of the spiral-shaped strip, the larger the total equivalent inductance, the more obvious the SSPP response, and the stronger the field confinement is. The conclusion in the figure is consistent with that obtained from Eq. (5), which verifies the accuracy of the proposed model.

Therefore, as shown in Fig. 5, the proposed SSPP in this paper achieves flexible dispersion control by changing the folded stepped groove and spiral-shaped structure, and further reduces the circuit size to a certain extent, achieving stronger field constraints.

Fabrication and Measurement

Based on the cell dispersion characteristics analyzed above, corresponding SSPP TL with low-pass filtering characteristics is designed. The transverse width of SSPP TL is reduced by adopting a folded stepped groove and a spiral-shaped structure. The schematic configuration of the transmission line is shown in Fig. 6, which consists of three parts: (I) CPW serves as the input/output port connected to the SMA connector for measurement, (II) the transition area from CPW to SSPP waveguide is used for mode conversion, and (III) the SSPP structure has a periodic arrangement of nine units.

In order to further quantitatively evaluate the performance of SSPP waveguides, we made a prototype as shown in Fig. 7, with the same parameters as the configuration in Fig. 2. Figure 8 shows the comparison between simulated and measured S-parameters at the cutoff frequency. At low

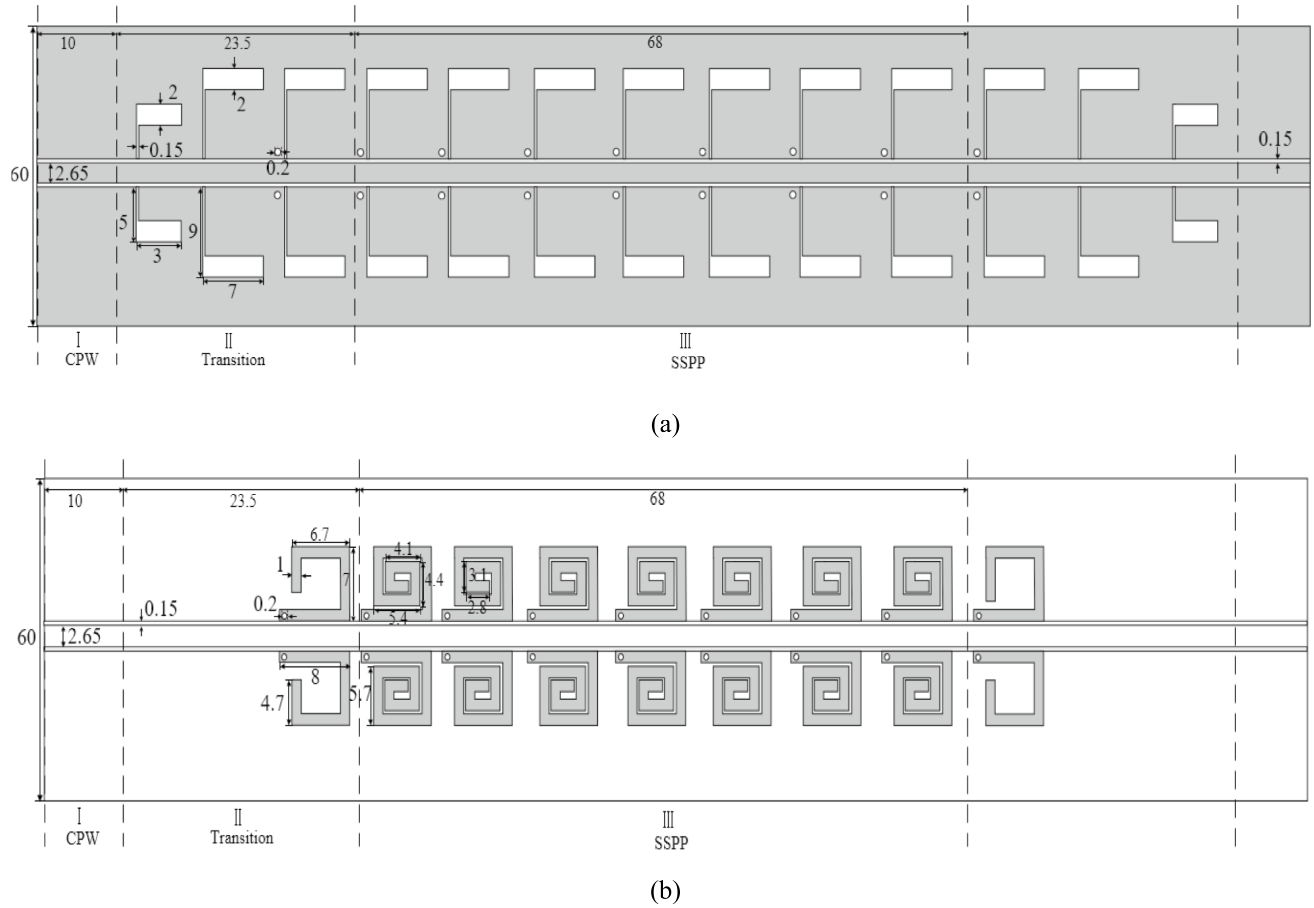

Fig. 6 The schematic configurations. **a** The top layout of the SSPP. **b** The bottom layout of the SSPP (dimensions in mm)

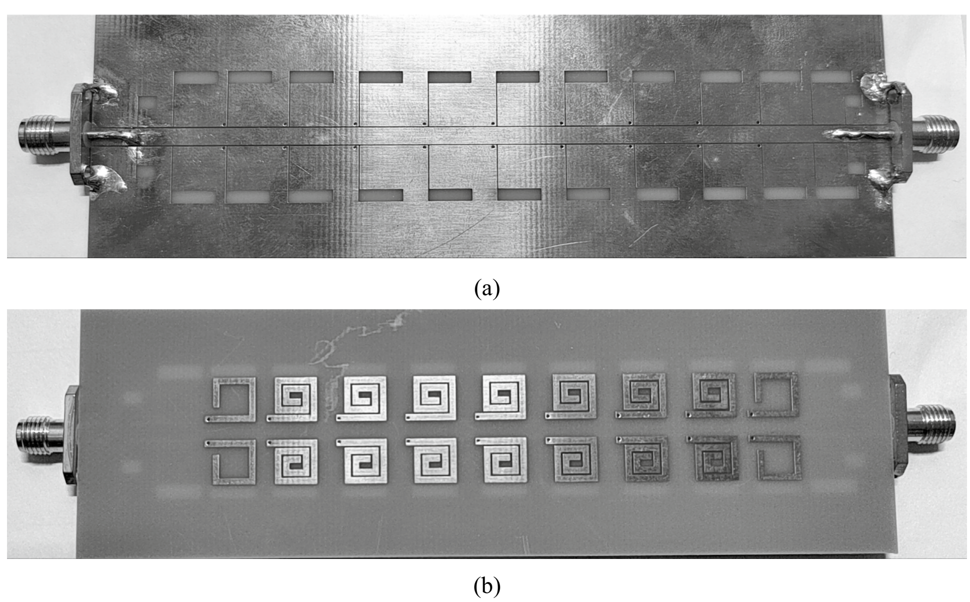

Fig. 7 **a** Top view of the fabricated CPW SSPP waveguide. **b** Bottom view of the fabricated CPW SSPP waveguide

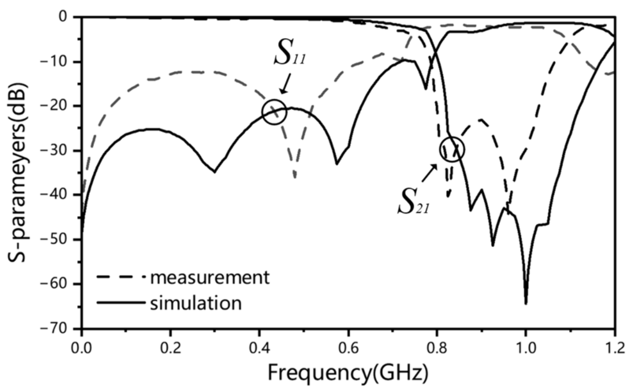

Fig. 8 Simulated and measured S-parameters

frequencies, the simulation results are in good agreement with the measured results, indicating that the proposed SSPP TL has excellent filtering characteristics consistent with the theoretical design, while occupying a relatively small volume. The difference between simulated and measured values is caused by factors such as manufacturing tolerances and measurement environment.

In addition, the proposed SSPP TL exhibits obvious filtering performance. To visualize the filtering performance of the proposed SSPP TL, the simulated electric field distributions of the SSPP TL are investigated in Fig. 9. It can be observed in Fig. 9 that in the pass frequency band the EM waves propagate smoothly along the TL, while in the reject frequency band, most of the waves are reflected.

In Table 1, we compared the proposed SSPP TL with some reported SSPP TLs in terms of asymptotic frequency f_a, groove shape, lateral width w_t, and period p. It is evident that the proposed SSPP TL has the narrowest lateral width, and the shortest p, insertion loss (IL), and return loss (RL). It is evident that the proposed SSPP TL has the narrowest lateral width, and the shortest p. In addition, by increasing the inductance brought by the bottom spiral-shaped structure, the size of the SSPP can be further reduced.

Table 1 Performance of previous works and this work

Ref	f_a (GHz)	Shape	w_t (λ_a)	p (λ_a)	IL (dB)	RL (dB)
[12]	8.9	Double layer	0.890	0.297	2.6	10
[13]	6.5	Fishbone	0.110	0.301	3	11.4
[14]	6.1	Zigzag	0.101	0.162	2.5	10
[15]	9	Smooth gradient	0.359	0.372	2	10
This work	0.81	Stepped	0.024	0.068	4	10

λ_a the wavelength at f_a, w_t the lateral width of SSPP TLs, p the period of SSPP TLs, *IL* insertion loss, *RL* return loss

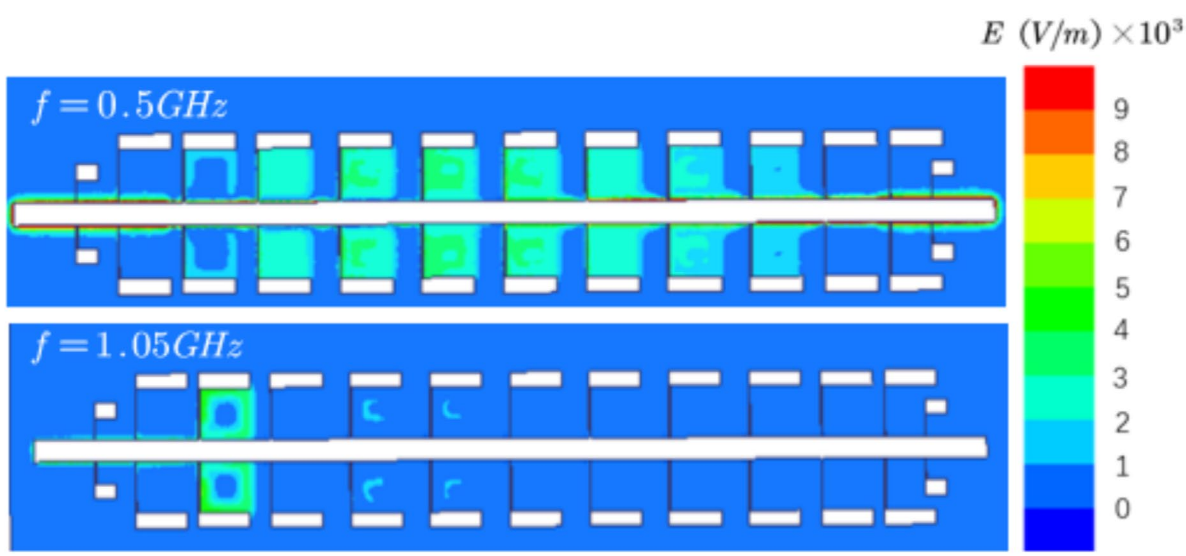

Fig. 9 Simulated E-field distributions of frequency in pass band and reject band along the proposed SSPP TL

Conclusion

This article proposes a novel SSPP TL based on the folded stepped groove and spiral-shaped structure. Research based on equivalent circuit models shows that the proposed SSPP has a lower asymptotic frequency, a stronger field confinement ability, and a smaller system size. In addition, by changing the folded stepped groove and spiral-shaped structure, the dispersion curve can be flexibly controlled. Finally, based on the proposed structure, a CPW SSPP TL is designed, manufactured, and tested to validate our design theory. The measurement results indicate that the structure has low asymptotic frequency and low-pass filtering characteristics, which is conducive to promoting the development and application of SSPPs.

Author Contributions All authors contributed to the study conception and design. The first draft of the manuscript was written by Y.-X.C. and all authors commented on previous versions of the manuscript. J.-Y.Z. prepared Figs. 4, 5, and 9. Y.-Y.K. wrote the conclusion. G.-P.Z. assisted in the completion of manuscript revision. Methodology, review, and editing were performed by L. L. All authors read and approved the final manuscript.

Data Availability No datasets were generated or analysed during the current study.

Declarations

Competing Interests The authors declare no competing interests.

References

1. Barnes WL, Dereux A, Ebbesen TW (2003) Surface plasmon subwavelength optics. Nature 424(6950):824–830. https://doi.org/10.1038/nature01937
2. Garcia-Vidal FJ, Martin-Moreno L, Pendry JB (2005) Surfaces with holes in them: new plasmonic metamaterials. J Opt A Pure Appl Opt 7(2):S97. https://doi.org/10.1088/1464-4258/7/2/013
3. Wei D, Li J, Yang J, Qi Y, Yang G (2018) Wide-scanning-angle leaky-wave array antenna based on microstrip SSPPs-TL. IEEE Antennas Wirel Propag Lett 17(8):1566–1570. https://doi.org/10.1109/LAWP.2018.2855178
4. Shen XP, Cui TJ (2013) Planar plasmonic metamaterial on a thin film with nearly zero thickness. Appl Phys Lett 102(21):211909. https://doi.org/10.1063/1.4808350
5. Williams CR, Andrews SR, Maier SA, Fernandez-Dominguez AI, Martin-Moreno L, Garcia-Vidal FJ (2008) Highly confined guiding of terahertz surface plasmon polaritons on structured metal surfaces. Nat Photonics 2(3):175–179. https://doi.org/10.1038/nphoton.2007.301
6. Kianinejad A, Chen ZN, Qiu C-W (2018) Full modeling, loss reduction, and mutual coupling control of spoof surface plasmon-based meander slow wave transmission lines. IEEE Trans Microw Theory Tech 66(8):3764–3772. https://doi.org/10.1109/TMTT.2018.2841857
7. Zhang HC, He PH, Tang WX, Luo Y, Cui TJ (2019) Planar spoof SPP transmission lines: applications in microwave circuits. IEEE Microwave Mag 20(11):73–91. https://doi.org/10.1109/MMM.2019.2935363
8. Gao X et al (2019) Crosstalk suppression based on mode mismatch between spoof SPP transmission line and microstrip. IEEE Transactions on Components, Packaging and Manufacturing Technology 9(11):2267–2275. https://doi.org/10.1109/TCPMT.2019.2931373
9. He PH, Zhang HC, Tang WX, Cui TJ (2018) Shielding spoof surface plasmon polariton transmission lines using dielectric box. IEEE Microw Wirel Compon Lett 28(12):1077–1079. https://doi.org/10.1109/LMWC.2018.2878968
10. He PH, Ren Y, Shao C, Zhang HC, Zhang LP, Cui TJ (2021) Suppressing high-power microwave pulses using spoof surface plasmon polariton mono-pulse antenna. IEEE Trans Antennas Propag 69(12):8069–8079. https://doi.org/10.1109/TAP.2021.3083836
11. Gao X, Cui TJ (2015) Spoof surface plasmon polaritons supported by ultrathin corrugated metal strip and their applications. Nanotechnol Rev 4(3):239–258. https://doi.org/10.1515/ntrev-2014-0032
12. Zu H-R, Wu B, Su T (2022) Beam manipulation of antenna with large frequency-scanning angle based on field confinement of spoof surface plasmon polaritons. IEEE Trans Antennas Propag 70(4):3022–3027. https://doi.org/10.1109/TAP.2021.3118739
13. Guo Y-J, Xu K-D, Cheng X, Deng X-J (2019) Review of some new spoof surface plasmon polariton waveguides. In: 2019 Photonics & Electromagnetics Research Symposium - Fall (PIERS - Fall). Xiamen, China, pp 2858–2864. https://doi.org/10.1109/PIERS-Fall48861.2019.9021711
14. He PH, Zhang HC, Gao XX, Niu LY, Tang WX et al (2019) A novel spoof surface plasmon polariton structure to reach ultra-strong field confinements. Opto-Electron Adv 2:190001. https://doi.org/10.29026/oea.2019.190001
15. Liang Y, Yu H, Wen J et al (2016) On-chip sub-terahertz surface plasmon polariton transmission lines with mode converter in CMOS. Sci Rep 6:30063. https://doi.org/10.1038/srep30063
16. Caloz C, Okabe H, Iwai T, Itoh T (2004) A simple and accurate model for microstrip structures with slotted ground plane. IEEE Microw Wirel Compon Lett 14(4):133–135. https://doi.org/10.1109/LMWC.2004.828725